

Atlantic Ocean CO₂ uptake reduced by weakening of the meridional overturning circulation

Fiz F. Pérez^{1*}, Herlé Mercier², Marcos Vázquez-Rodríguez¹, Pascale Lherminier³, Anton Velo¹, Paula C. Pardo¹, Gabriel Rosón⁴ and Aida F. Ríos¹

Uptake of atmospheric carbon dioxide in the subpolar North Atlantic Ocean declined rapidly between 1990 and 2006. This reduction in carbon dioxide uptake was related to warming at the sea surface, which—according to model simulations—coincided with a reduction in the Atlantic meridional overturning circulation. The extent to which the slowdown of this circulation system—which transports warm surface waters to the northern high latitudes, and cool deep waters south—contributed to the reduction in carbon uptake has remained uncertain. Here, we use data on the oceanic transport of volume, heat and carbon dioxide to track carbon dioxide uptake in the subtropical and subpolar regions of the North Atlantic Ocean over the past two decades. We separate anthropogenic carbon from natural carbon by assuming that the latter corresponds to a pre-industrial atmosphere, whereas the remaining is anthropogenic. We find that the uptake of anthropogenic carbon dioxide—released by human activities—occurred almost exclusively in the subtropical gyre. In contrast, natural carbon dioxide uptake—which results from natural Earth system processes—dominated in the subpolar gyre. We attribute the weakening of contemporary carbon dioxide uptake in the subpolar North Atlantic to a reduction in the natural component. We show that the slowdown of the meridional overturning circulation was largely responsible for the reduction in carbon uptake, through a reduction of oceanic heat loss to the atmosphere, and for the concomitant decline in anthropogenic CO₂ storage in subpolar waters.

Contemporary CO₂ uptake from the atmosphere by the global ocean has been estimated to be $1.6 \pm 0.9 \text{ PgC yr}^{-1}$ from an observation-based CO₂ flux climatology¹ referenced to the year 2000. Contemporary atmospheric CO₂ consists of a mix of molecularly identical natural and anthropogenic CO₂ (C_{ANT}). The whole North Atlantic (from the Equator to the Bering Strait, including the Arctic seas) represents only 13% of the global ocean area and yet annually accounts for about one-third of the contemporary ocean CO₂ uptake (0.47 PgC yr^{-1}) and has the largest of C_{ANT} storage rates ($0.49 \pm 0.04 \text{ PgC yr}^{-1}$ referenced to 2004) of all oceans². However, air–sea CO₂ uptake in the North Atlantic is not necessarily predominantly anthropogenic^{3,4}. In fact, air–sea CO₂ fluxes in the North Atlantic result from anthropogenic forcing and progressive northward cooling of the upper limb of the meridional overturning circulation (MOC). The latter is responsible for the North Atlantic uptake of natural CO₂ (ref. 5) that would occur even in the absence of the anthropogenic forcing. This air–sea flux of natural CO₂ is driven by thermal processes⁵—not biological processes—and has been estimated to be $0.31\text{--}0.39 \text{ PgC yr}^{-1}$ (refs 5,6), which represents roughly three-quarters of the contemporary air–sea CO₂ uptake. The remaining uptake ($0.08\text{--}0.16 \text{ PgC yr}^{-1}$) comes from the anthropogenic perturbation, which alone cannot account for the C_{ANT} storage rate of the North Atlantic (ref. 2). The other source of C_{ANT} comes from the northward transport of C_{ANT} -laden south-latitude waters^{4,7–9} by the upper limb of the MOC. Air–sea CO₂ fluxes in the subpolar and subtropical regions have similar rates (0.27 and 0.22 PgC yr^{-1} , referenced to 2000, respectively¹), but the flux per unit area in the subpolar North Atlantic is twice that in

the subtropical North Atlantic (2.0 versus $1.0 \text{ mol C m}^{-2} \text{ yr}^{-1}$). At multi-decadal timescales, sea-surface $p\text{CO}_2$ trends in these regions follow the atmospheric increase¹. However, these two regions also have contrasting responses to different North Atlantic Oscillation (NAO) periods. The Hurrell NAO winter index is computed as the difference in the surface atmospheric pressure between Iceland and Azores (time series values available at www.cgd.ucar.edu/cas/jhurrell/indices.html). In the early 1990s (1989–1995) the 5-year mean \pm standard deviation of this index was 3.3 ± 0.8 , indicating a high phase of the NAO. A low-NAO phase period followed during the years 2002–2006, when the index value dropped to -0.1 ± 0.6 . Between 1993 and 2006, the CO₂ uptake rate in the western subpolar¹⁰ and, more generally, in the subpolar gyre¹¹ markedly weakened as evidenced by the rapid increase in sea-surface $p\text{CO}_2$ compared with atmospheric $p\text{CO}_2$. Changes in the NAO and the associated weakening of the northward transport of subtropical water by the North Atlantic Current (NAC) have been identified, using inverse atmospheric CO₂ and physical–biological models^{12,13}, as the main causes for the decrease in CO₂ uptake in the subpolar North Atlantic. In contrast, in the subtropical North Atlantic, CO₂ uptake increased during the years with a low NAO index^{14,15}. There are, however, few observations of C_{ANT} transport reported for different NAO conditions. In addition, numerical models have shown contrasting CO₂ uptake responses^{13,16} and discrepancies with field data, suggesting that more observations are required to better understand the interactions between ocean circulation and the carbon cycle, in particular regarding the mechanisms governing the exchange, advection and accumulation of CO₂.

¹Instituto de Investigaciones Marinas, IIM-CSIC, 36208 Vigo, Spain, ²CNRS, Laboratoire de Physique des Océans, UMR6523, CNRS, Ifremer, IRD, UBO, 29280 Plouzané, France, ³Ifremer, Laboratoire de Physique des Océans, UMR6523, CNRS, Ifremer, IRD, UBO, 29280 Plouzané, France, ⁴Faculty of Marine Sciences, University of Vigo, Campus Lagoas-Marcosende, 36200 Vigo, Spain. *e-mail: fiz.perez@iim.csic.es.

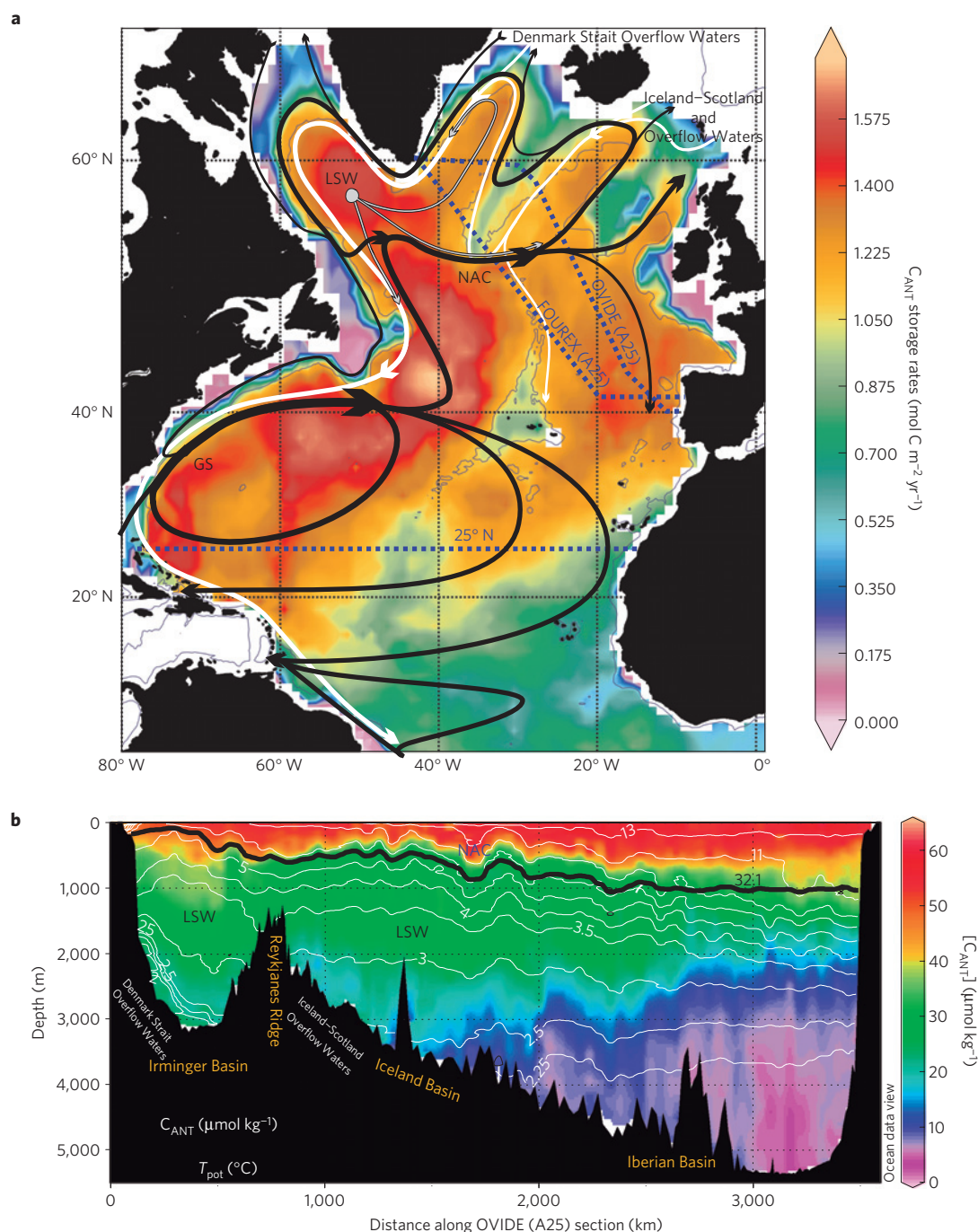


Figure 1 | Circulation and C_{ANT} in the North Atlantic. **a**, C_{ANT} storage rates ($\text{mol C m}^{-2} \text{ yr}^{-1}$) and the main currents and water masses participating in the MOC (black line: NAC, Gulf Stream; grey line: LSW; white lines: Denmark Strait and Iceland-Scotland Overflow Waters). The 25°N , FOUREX and OVIDE section tracks are indicated (blue dotted lines). **b**, Vertical distribution of $[C_{ANT}]$ ($\mu\text{mol kg}^{-1}$) during the OVIDE 2004 cruise. Potential temperature ($^\circ\text{C}$; white lines) and the isopycnal $\sigma_1 = 32.10$ (solid black line) separating the upper and lower limbs of MOC are also shown.

CO_2 transport by the MOC

The analysis of repeated trans-Atlantic sections at 25°N showed that the upper limb of the MOC carries $18.7 \pm 2.1 \text{ Sv}$ ($\text{Sv} = 10^6 \text{ m}^3 \text{ s}^{-1}$) northwards¹⁷ (northward transport is considered positive). Most of this transport occurs through the Gulf Stream and, downstream, through the NAC (Fig. 1). The warm water moving northwards in the upper limb of the MOC has high concentrations of C_{ANT} ($[C_{ANT}]$), whereas the cold, deep water moving southwards^{4,7} has very low $[C_{ANT}]$. This pattern yields net northward transports of heat¹⁸ and C_{ANT} of $1\text{--}1.3 \text{ PW}$ and $0.19\text{--}0.23 \text{ PgC yr}^{-1}$ (refs 4, 7), respectively. The overturning and the southward transport of deep

water of the MOC happen in the northern North Atlantic and Nordic seas, where high wintertime heat loss generates vertical convection and produces cold, fresh and well-ventilated deep waters¹⁹ that are entrained in the deep western boundary current. Recent estimations of the MOC across the repeated A25 section (Greenland to Portugal; Fig. 1) showed slightly weaker mass transports^{20,21} ($12\text{--}18.5 \text{ Sv}$) than at 25°N . The upper and lower limbs of the MOC showed contrasting temperatures and $[C_{ANT}]$ (Fig. 1b, see Methods for details on C_{ANT} computations), but both properties are positively correlated. The small westward increase in $[C_{ANT}]$ at constant temperature indicates recent ventilation of

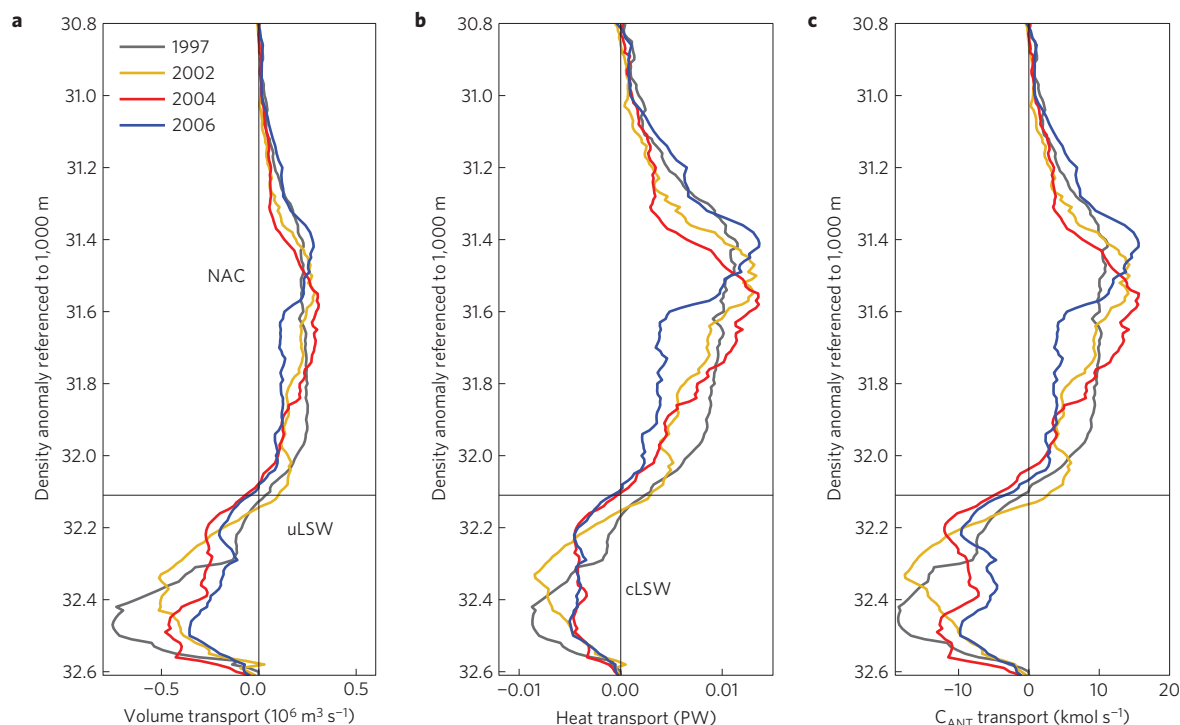


Figure 2 | Integrated transports of volume, heat and C_{ANT} across the A25 section (Greenland–Portugal) in 0.01 density bins. **a, Volume transport ($10^6 \text{ m}^3 \text{ s}^{-1}$). **b**, Heat transport (PW). **c**, C_{ANT} transport (kmol s^{-1}). The coloured lines refer to years 1997 (grey), 2002 (yellow), 2004 (red) and 2006 (blue). The $\sigma_1 = 32.10$ horizon (solid black horizontal lines) represents the boundary between the upper and lower limbs of the MOC. NAC, North Atlantic Current; uLSW, upper LSW; cLSW, classical LSW.**

the western side of the section. In the surface layer, $[C_{ANT}]$ is close to saturation. East of the NAC, the low values ($< 10 \mu\text{mol kg}^{-1}$) in deep waters create a larger vertical gradient of C_{ANT} between the surface and the deep ocean than to the west of the NAC, that is in the subpolar region, where the Labrador Sea Water (LSW), the Denmark Strait Overflow Water and the Iceland–Scotland Overflow Water show moderate $[C_{ANT}]$.

Numerical models have shown that NAO conditions influence air–sea CO_2 uptake in the North Atlantic (ref. 12) by modulating the strength with which the NAC carries subtropical waters into the subpolar gyre¹³. However, these results have not been confronted with measurements of volume, heat and CO_2 transports owing to the lack of observations during different NAO conditions. We examined several occupations of the A25 Greenland–Portugal section (Fig. 1a) conducted in August 1997 (FOUREX cruise) and in June 2002, 2004 and 2006 (OVIDE cruises). The year 1997 came after an unusually long high-NAO period followed by a period of lower NAO between 2002 and 2006. The A25 cruise was specifically designed to run perpendicularly across the main North Atlantic currents (the different branches of the NAC and the boundary currents linked to the topography) to minimize the transports due to eddies²². Measurements from these cruises were used to calculate MOC_σ transport^{20,21,23}, taking σ_1 (density anomaly referenced to 1,000 dbar) as the vertical coordinate (Fig. 2). MOC_σ varied from $20.5 \pm 2.2 \text{ Sv}$ in 1997 to the average value of $14.6 \pm 1.7 \text{ Sv}$ for the 2002–2006 period (see Methods and Supplementary Information for details on the removal of the seasonal cycle and the computation of the uncertainties). When integrated from Greenland to Portugal along constant σ_1 -lines, heat and C_{ANT} transports resemble the vertical profiles of the overturning circulation (Fig. 2). Volume, heat and C_{ANT} transport profiles are highly correlated ($0.92 > r^2 > 0.89$), because the upper limb of the MOC transports warmer waters with higher $[C_{ANT}]$ than the lower limb. On average, the net volume transport

is negligible, and there is a net northward transport of heat ($0.59 \pm 0.09 \text{ PW}$) and C_{ANT} ($0.092 \pm 0.010 \text{ PgC yr}^{-1}$). In 1997, the circulation showed a strong southward volume transport at intermediate levels ($32.4 < \sigma_1 < 32.5$) that corresponds to the layer of the classical LSW (Fig. 2). On the other hand, during the lower NAO period, the southward volume transport was slightly stronger in the layer of the upper LSW ($32.2 < \sigma_1 < 32.3$; ref. 19). In addition, the upper limb of MOC_σ ($\sigma_1 < 32.1$) showed a stronger transport in 1997 than in 2002–2006 (Fig. 2a), which is attributed to the NAC variability²³. The heat and C_{ANT} transports in 2002–2006 ($0.41 \pm 0.06 \text{ PW}$ and $0.074 \pm 0.009 \text{ PgC yr}^{-1}$) were lower than in 1997 ($0.76 \pm 0.09 \text{ PW}$ and $0.110 \pm 0.012 \text{ PgC yr}^{-1}$). Most remarkably, although the weakening of MOC_σ and of C_{ANT} transport were very similar (29 and 33%, respectively), heat transport underwent a more pronounced reduction (46%) between 1997 and 2002–2006. This contrasting behaviour of volume and heat transports agrees with results from high-resolution circulation models²⁴. We will treat the observations obtained in 1997 as a case study of circulation linked to a high-NAO period, as opposed to the measurements obtained during 2002–2006 that were associated with a low/neutral-NAO period.

Anthropogenic CO_2 budget of the North Atlantic

The C_{ANT} budget of any oceanic region is the result of the balance between lateral advection, air–sea fluxes and storage rates. Hereafter, we will refer to the North Atlantic as the region extending from 25° N to the Bering Strait. We calculated the North Atlantic C_{ANT} budget referenced to 2004 from updated data sets and for four different subregions or boxes (Fig. 3). In the subtropical box, the C_{ANT} storage rate was computed as described in the Methods, whereas the estimates in other boxes were obtained from the literature (Supplementary Information). For the North Atlantic, we obtained a storage rate of $0.386 \pm 0.012 \text{ PgC yr}^{-1}$ ($0.95 \pm 0.05 \text{ mol C m}^{-2} \text{ yr}^{-1}$) consistent with previous results ($0.39 \pm 0.02 \text{ PgC yr}^{-1}$,

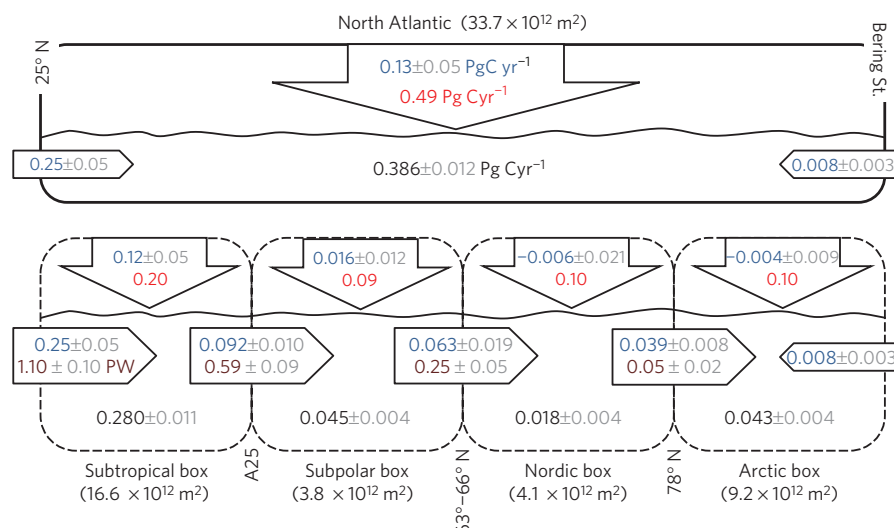


Figure 3 | C_{ANT} budget in the North Atlantic referenced to 2004. The upper panel represents the North Atlantic and the lower panels represent the four subregions. The horizontal arrows show the lateral transports of C_{ANT} in PgC yr^{-1} (blue font) and heat transports in petawatts (brown font). The black numbers in the panels are the C_{ANT} storage rates in PgC yr^{-1} . The vertical arrows show the anthropogenic (numbers in blue font) and contemporary (red font) air-sea CO_2 fluxes in PgC yr^{-1} . Errors appear in grey font. The surface area (m^2) of each box and the latitudinal boundaries between them are shown.

referenced to 2004; ref. 25). The C_{ANT} transports at 25°N (refs 4,7) were updated from 1992 and 1998 to 2004, resulting in a mean value of $0.25 \pm 0.05 \text{ PgC yr}^{-1}$ (Methods) that is consistent with a long-term average MOC (ref. 17). Comparatively, C_{ANT} transport in the Bering Strait is low ($0.008 \pm 0.003 \text{ PgC yr}^{-1}$; refs 7,25). Closing the C_{ANT} budget in the North Atlantic, an air-sea C_{ANT} flux of $0.13 \pm 0.05 \text{ PgC yr}^{-1}$ was inferred. This estimate is compatible with the value of $0.17 \pm 0.06 \text{ PgC yr}^{-1}$ (rescaled to 2004) derived from $\delta^{13}\text{C}$ observations⁹. Overall, these results indicate that the net advective transports contribute to $65 \pm 13\%$ of the North Atlantic C_{ANT} storage rate (Fig. 3). Importantly, our observation-based estimate of the contribution of lateral transports to the C_{ANT} storage rate is larger than the 30% obtained by ocean inversions that combine C_{ANT} observations with transports and mixing from general circulation models²⁵. By way of contrast, our result is consistent with a biogeochemical model²⁶ that predicted larger northward C_{ANT} transports than ocean inversions in the North Atlantic. Subtracting our estimate of air-sea C_{ANT} flux from the contemporary CO_2 uptake for the North Atlantic (0.49 PgC yr^{-1} ; ref. 1), we obtained a natural CO_2 uptake of 0.36 PgC yr^{-1} , thereby corroborating independent estimates^{5,6}. The air-sea C_{ANT} flux represents about 26% of the contemporary air-sea CO_2 uptake, which is much smaller than the 63% obtained from oceanic inversions³. The relevance of our result is that the air-sea C_{ANT} and natural CO_2 uptake estimates from the C_{ANT} budget are consistent with independent $^{13}\text{C}/^{12}\text{C}$ observations⁹ and with other estimates of the air-sea natural CO_2 uptake^{5,6}.

The C_{ANT} storage rate estimated for the subtropical box is $0.280 \pm 0.011 \text{ PgC yr}^{-1}$ ($1.41 \pm 0.05 \text{ mol C m}^{-2} \text{ yr}^{-1}$). Thus, the subtropical box contributes 73% of the North Atlantic C_{ANT} storage rate, even though it represents only 49% of the North Atlantic area. By closing the C_{ANT} budget for this box (Fig. 3), we inferred an air-sea C_{ANT} uptake of $0.12 \pm 0.05 \text{ PgC yr}^{-1}$ ($0.60 \pm 0.25 \text{ mol C m}^{-2} \text{ yr}^{-1}$). Here, the air-sea C_{ANT} flux is predominant in the contemporary air-sea CO_2 flux ($1.0 \text{ mol C m}^{-2} \text{ yr}^{-1}$). It represents 92% of the North Atlantic air-sea C_{ANT} uptake. In contrast, in the subpolar box, the C_{ANT} storage rate per unit area ($0.99 \pm 0.06 \text{ mol C m}^{-2} \text{ yr}^{-1}$) amounts to $\sim 70\%$ of that in the subtropical box²⁷. To derive the C_{ANT} budget for the subpolar box, the C_{ANT} lateral transport over the Nordic sills ($0.063 \pm 0.019 \text{ PgC yr}^{-1}$) was calculated from available

volume transports^{21,28} and from $[C_{ANT}]$ estimated from water mass ages and mixing models²⁹ (Supplementary Information). Then, the air-sea C_{ANT} flux was estimated to be $0.016 \pm 0.012 \text{ PgC yr}^{-1}$, which represents 35% of the C_{ANT} storage rate in this box. The air-sea C_{ANT} flux per unit area in the subpolar box ($0.36 \pm 0.25 \text{ mol C m}^{-2} \text{ yr}^{-1}$) is about 60% of the subtropical box, which gives the subtropical box a prevailing role in C_{ANT} uptake. Furthermore, the contemporary air-sea CO_2 uptake per unit area ($2.0 \text{ mol C m}^{-2} \text{ yr}^{-1}$) in the subpolar box is five times higher than the air-sea C_{ANT} uptake. This means that the natural component largely prevails over the anthropogenic component in the subpolar box. Interestingly, this result is in contrast with the subtropical box, where the air-sea anthropogenic flux is the main component ($\sim 60\%$).

The net heat and C_{ANT} transports flowing into the Nordic seas reach $0.25 \pm 0.05 \text{ PW}$ and $0.063 \pm 0.019 \text{ PgC yr}^{-1}$, respectively (Fig. 3 and Supplementary Information). The C_{ANT} lateral transport almost fully accounts for the C_{ANT} storage rate in the Nordic³⁰ and Arctic seas³¹, meaning that air-sea C_{ANT} fluxes are practically zero (Fig. 3). Analyses based on $^{13}\text{C}/^{12}\text{C}$ measurements^{32,33} have determined that the upper waters entering the Nordic seas are saturated with C_{ANT} , preventing any further C_{ANT} uptake from the atmosphere and possibly causing outgassing owing to the decline in buffering capacity. The strong air-sea heat loss in the Nordic and Arctic seas actually drives the uptake of natural CO_2 , as corroborated by observations in climatological analyses¹ that indicate a high air-sea CO_2 uptake ($2.0 \text{ mol C m}^{-2} \text{ yr}^{-1}$) north of 50°N . In summary, whereas heat loss causes a strong natural CO_2 uptake in the Nordic and Arctic regions, the low anthropogenic component is less affected by the air-sea heat fluxes.

NAO impact on CO_2 fluxes

The subpolar gyre is a remarkably rapid entrance portal for C_{ANT} into the deep ocean owing to deep convection. In the early 1990s, the highly positive NAO period coincided with exceptional convection activity in the Labrador^{19,34} and Irminger³⁵ seas. Between 1997 and 2003, lower LSW formation rates prompted a decrease of 20 mol C m^{-2} in the C_{ANT} inventory, as inferred from chlorofluorocarbon data³⁶. In the subpolar box, the C_{ANT} storage rate dropped from 0.083 ± 0.008 during high-NAO conditions in 1997 to $0.026 \pm 0.004 \text{ PgC yr}^{-1}$ during the 2002–2006 low-NAO period²⁷. Hence, C_{ANT} storage rates per unit area were nearly three

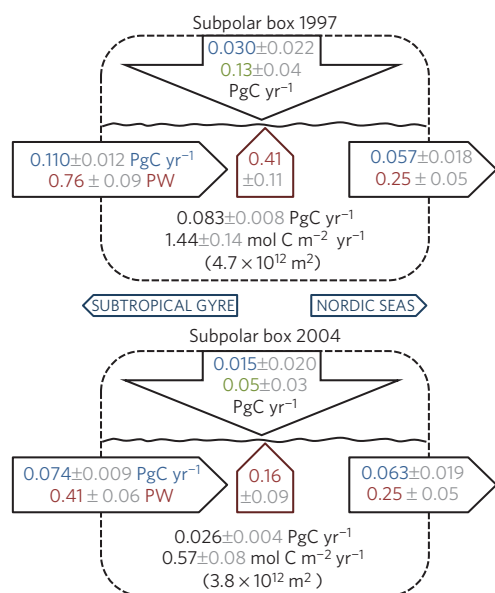


Figure 4 | Variability of the C_{ANT} budget in the subpolar box during high NAO (1997) and low NAO (2002–2006). The arrow and number formats are the same as in Fig. 3, except for the numbers in green font that are the natural air-sea CO_2 fluxes in PgC yr^{-1} , and in maroon font that are the air-sea heat flux in petawatts. Areal C_{ANT} storage rates ($\text{mol C m}^{-2} \text{yr}^{-1}$) are also given. For 1997, the heat budget includes a heat accumulation rate of 0.10 ± 0.05 PW.

times lower during low-NAO than high-NAO periods (Fig. 4). The decrease in northward C_{ANT} transport (Fig. 4) that followed the high-to-low NAO transition (from 0.110 to $0.074 \text{ PgC yr}^{-1}$) is strongly related to the weakening of the intensity of the MOC (from 20.5 ± 2.2 to $14.6 \pm 1.7 \text{ Sv}$). Most remarkably, the converging C_{ANT} lateral transports in the subpolar box decreased from 0.053 ± 0.021 to $0.011 \pm 0.020 \text{ PgC yr}^{-1}$. In these estimations, we assumed that the volume transport over the Nordic sills was constant, as suggested by observations²⁸, and $[C_{ANT}]$ was time-rescaled using a rate of increase of $1.6\% \text{ yr}^{-1}$ (Supplementary Information). After these calculations, the inferred air-sea C_{ANT} flux for the subpolar region was $0.53 \pm 0.22 \text{ mol C m}^{-2} \text{yr}^{-1}$ during the high-NAO period and $0.33 \pm 0.25 \text{ mol C m}^{-2} \text{yr}^{-1}$ during the low-NAO period. During the low-NAO period, the C_{ANT} storage rate decreased owing to the decrease in C_{ANT} lateral transport associated with the weakening of the MOC. Our results also suggest that this decrease was associated with a weakening in the air-sea C_{ANT} uptake.

The variability of the air-sea CO_2 flux in the subpolar gyre has already been described, modelled and discussed in regard to NAO variability^{12,13,37,38}. In the northwestern subpolar gyre, a reduction in the contemporary air-sea CO_2 flux of $\sim 1.2 \text{ mol C m}^{-2} \text{yr}^{-1}$ was observed between 1993–1994 and 2003–2005 (refs 11,37) and numerical simulation linked it to the weakening of the advection of subtropical waters with low total inorganic CO_2 (C_T) into the subpolar gyre¹³. This weakening is in agreement with our results (Fig. 4). During high-NAO periods, heat loss increased³⁹, favouring the decrease in the surface $p\text{CO}_2$. The opposite is true during low-NAO periods. Assuming a constant heat flux of $0.25 \pm 0.05 \text{ PW}$ over the sills²⁸, we inferred, from the heat budget, a heat loss that is 1.5–3 times higher during high-NAO than during low-NAO periods (Fig. 4). Using the relationship between heat loss and natural CO_2 flux (see Methods), we inferred a decrease in the air-sea flux of natural CO_2 of 3.0 ± 1.0 to $1.7 \pm 1.0 \text{ mol C m}^{-2} \text{yr}^{-1}$ (0.13 – 0.05 PgC yr^{-1} ; Fig. 4). This estimate is compatible with the rate of decrease in air-sea

CO_2 fluxes in the subpolar gyre (2.3 – $1.0 \text{ mol C m}^{-2} \text{yr}^{-1}$) reported from surface observations³⁸. Most importantly, this result strongly suggests that variability in the air-sea flux of natural CO_2 over the subpolar gyre responds to variability in the advection of subtropical waters with low $[C_T]$ and can be determined from the air-sea heat flux.

A possible explanation for the contrasting behaviour of the subtropical and subpolar regions lies in the origin of the water masses crossing the Florida Strait where $\sim 45\%$ of the volume transport comes from the South Atlantic as warm and intermediate waters⁴⁰ with low $[C_{ANT}]$ (ref. 4). These low- $[C_{ANT}]$ waters are part of the upper limb of the MOC and reach C_{ANT} saturation levels on their path to the subpolar gyre. They incorporate about 0.08 PgC yr^{-1} , which represents two-thirds of the air-sea C_{ANT} flux in the subtropical box and contributes to the local response to anthropogenic forcing (Fig. 3). This explains why the air-sea C_{ANT} flux in the subtropical region is higher than that observed in the subpolar region. Furthermore, the intermediate water flowing through the Florida Strait is oversaturated with natural CO_2 ($\sim 30 \mu\text{mol kg}^{-1}$) owing to biological remineralization⁴. This allows the waters in the upper limb of the MOC to remain CO_2 -saturated with low additional atmospheric uptake, despite the $\sim 7^\circ \text{C}$ cooling undergone as they travel through the subtropical box, thereby explaining the low natural air-sea CO_2 flux in this box.

Our results give a coherent and observation-based understanding of the CO_2 budget in North Atlantic regions. Our analysis provides evidence that the air-sea C_{ANT} flux contribution to the C_{ANT} storage and to the total air-sea CO_2 flux in the North Atlantic is lower than expected from ocean inversions. Advection is the main contribution to the C_{ANT} storage rate north of 25°N . Practically, the entire air-sea C_{ANT} uptake in the North Atlantic occurs in the subtropical region, where the contemporary air-sea CO_2 flux is mainly anthropogenic, whereas the natural component predominates in the subpolar region. The high-to-low NAO transition was followed by a decrease in the heat and C_{ANT} transports into the subpolar region due to the weakening of the MOC and the simultaneous decrease in the C_{ANT} storage rate. As the anthropogenic contribution is a minor component of the contemporary air-sea CO_2 uptake in the subpolar region, we attribute the weakening of the contemporary air-sea CO_2 uptake to the decrease in natural CO_2 uptake. Our estimate of the decrease in natural CO_2 uptake inferred from the heat budget is in agreement with independent surface observations.

Finally, our study suggests that the long-term prediction of a reduction in the intensity of the MOC would be a positive climate-carbon feedback leading to a decrease in the C_{ANT} storage. Concomitant air-sea heat-loss reduction may lead to a decrease in the abiotic component of the natural CO_2 uptake, which would be an even more important feedback.

Methods

C_{ANT} estimations. $[C_{ANT}]$ was computed using the back-calculation φC_T^* method^{41,42} with an overall uncertainty of $\pm 5.2 \mu\text{mol kg}^{-1}$. $[C_{ANT}]$ in the subtropical region was estimated using the gridded CARINA (carbon dioxide in the Atlantic Ocean) data set⁴³ and applying the φC_T^* , TrOCA (tracer combining oxygen, inorganic carbon and total alkalinity; ref. 44) and TTD (transit time distribution; ref. 45) methods. C_{ANT} storage rates obtained from each of these methods were in good agreement. The final C_{ANT} storage rate and its uncertainty for the subtropical region were calculated as the mean and the standard deviation of C_{ANT} storage rates obtained from each method. For the subpolar, Nordic and Arctic boxes, the storage rates were from refs 27,30,46, respectively. Further details are provided in the Supplementary Information.

Transport computations across A25. Absolute geostrophic currents were estimated using an inverse model constrained by subsurface acoustic Doppler current profiler measurements and an overall mass conservation constraint^{20,21,23}. The absolute velocity field is consistent with independent altimetry measurements²³ and estimates of the western boundary current transport⁴⁷ at the time of the OVIDE cruises. They are representative of the month of the cruise²² and the seasonal

variability was removed as explained in the Supplementary Information. Heat and C_{ANT} transports were calculated from current velocities perpendicular to the sections and from the potential temperature and C_{ANT} fields, respectively. The uncertainties of the MOC, heat and C_{ANT} transports were estimated to be ± 2 Sv, 0.05 PW and 0.014 PgC yr⁻¹, respectively (see Supplementary Information for full calculation details).

The errors of the mean transports (volume, heat or C_{ANT}) across the A25 section were calculated as the standard deviation of the transport values divided by the square root of the number of transport values included in the estimate. As only one transport estimate was available for the high-NAO conditions, the error equals the standard deviation of the transports between 1997 and 2006, after removing a linear trend.

C_{ANT} transport at 25° N. We used the estimates of C_{ANT} transports across 25° N reported in refs 4,7 that were respectively obtained from hydrographic cruises carried out in 1992 and 1998 and from C_{ANT} estimates based on a classic back-calculation method and on the C^* method. We rescaled both estimates to the year 2004 by removing the effect of the inter-annual variability of the MOC in C_{ANT} transports along 25° N. In addition, we corrected the MOC estimates for their intra-annual variability. The resulting value obtained after the rescaling was 0.25 ± 0.05 PgC yr⁻¹. Details on these computations and the uncertainty estimates are given in the Supplementary Information.

Relationship between air–sea fluxes of heat and natural CO₂. The linear regression of natural C_T transports versus heat transports reported in Supplementary Table S4 for the A25 line has a slope of -0.56 ± 0.10 PgC yr⁻¹ per petawatt ($P < 0.05$). Assuming that the variability of heat and natural C_T transports over the sills and of accumulative terms are negligible^{28,48}, this slope can be interpreted as a relationship between the air–sea flux of natural CO₂ and the air–sea heat loss in the subpolar box. In the Nordic seas, a similar relationship is found between air–sea flux of natural CO₂ and air–sea heat loss. Using the mean value of the observed air–sea CO₂ uptake (0.09 ± 0.01 and 0.11 ± 0.06 PgC yr⁻¹ as reported in refs 1,49, respectively) and the heat loss given in Fig. 3, we obtained a value of -0.5 ± 0.1 PgC yr⁻¹ of air–sea flux per petawatt of heat loss in the Nordic seas. This relationship can also be applied to the natural CO₂ air–sea fluxes of the Nordic seas, because here the C_{ANT} air–sea flux is negligible, as shown in Fig. 3.

Received 1 August 2012; accepted 23 November 2012;
published online 13 January 2013

References

1. Takahashi, T. *et al.* Climatological mean and decadal change in surface ocean pCO₂, and net sea-air CO₂ flux over the global oceans. *Deep-Sea Res. II* **56**, 554–577 (2009).
2. Sabine, C. L. *et al.* The oceanic sink for anthropogenic CO₂. *Science* **305**, 367–371 (2004).
3. Gruber, N. *et al.* Oceanic sources, sinks, and transport of atmospheric CO₂. *Glob. Biogeochem. Cycles* **23**, GB1005 (2009).
4. Rosón, G., Ríos, A. F., Pérez, F. F., Lavin, A. & Bryden, H. L. Carbon distribution, fluxes, and budgets in the subtropical North Atlantic Ocean (24.5°N). *J. Geophys. Res.* **108**, 3144 (2003).
5. Keeling, R. F. & Peng, T.-H. Transport of heat, CO₂ and O₂ by the Atlantic's thermohaline circulation. *Phil. Trans. R. Soc. Lond. B* **348**, 133–142 (1995); **348**, 133–142 (1995).
6. Mikaloff-Fletcher, S. E. *et al.* Inverse estimates of the oceanic sources and sinks of natural CO₂ and the implied oceanic carbon transport. *Glob. Biogeochem. Cycles* **21**, GB1010 (2007).
7. Macdonald, A. M., Baringer, M. O., Wanninkhof, R., Lee, K. & Wallace, D. W. R. A 1998–1992 comparison of inorganic carbon and its transport across 24.5° N in the Atlantic. *Deep-Sea Res. II* **50**, 3041–3064 (2003).
8. Álvarez, M., Ríos, A. F., Pérez, F. F., Bryden, H. L. & Rosón, G. Transports and budgets of total inorganic carbon in the subpolar and temperate North Atlantic. *Glob. Biogeochem. Cycles* **17**, 1002 (2003).
9. Quay, P. *et al.* Anthropogenic CO₂ accumulation rates in the North Atlantic Ocean from changes in the ¹³C/¹²C of dissolved inorganic carbon. *Glob. Biogeochem. Cycles* **21**, GB1009 (2007).
10. Metzl, N. *et al.* Recent acceleration of the sea surface fCO₂ growth rate in the North Atlantic subpolar gyre (1993–2008) revealed by winter observations. *Glob. Biogeochem. Cycles* **24**, GB4004 (2010).
11. Watson, A. J. *et al.* Tracking the Variable North Atlantic Sink for Atmospheric CO₂. *Science* **326**, 1391–1393 (2009).
12. Patra, P. K. *et al.* Interannual and decadal changes in the sea-air CO₂ flux from atmospheric CO₂ inverse modeling. *Glob. Biogeochem. Cycles* **19**, GB4013 (2005).
13. Thomas, H. *et al.* Changes in the North Atlantic Oscillation influence CO₂ uptake in the North Atlantic over the past 2 decades. *Glob. Biogeochem. Cycles* **22**, GB4027 (2008).
14. Gruber, N., Keeling, C. D. & Bates, N. R. Interannual variability in the North Atlantic ocean carbon sink. *Science* **298**, 2374–2378 (2002).
15. Bates, N. R. Interannual variability of the oceanic CO₂ sink in the subtropical gyre of the North Atlantic Ocean over the last 2 decades. *J. Geophys. Res.* **112**, C09013 (2007).
16. Ullman, D. J., McKinley, G. A., Bennington, V. & Dutkiewicz, S. Trends in the North Atlantic carbon sink: 1992–2006. *Glob. Biogeochem. Cycles* **23**, GB4011 (2009).
17. Kanzow, T. *et al.* Seasonal variability of the Atlantic meridional overturning circulation at 26.5° N. *J. Clim.* **23**, 5678–5698 (2010).
18. Bryden, H. L., Longworth, H. R. & Cunningham, S. A. Slowing of the Atlantic meridional overturning circulation at 25° N. *Nature* **438**, 655–657 (2005).
19. Yashayaev, I. & Dickson, B. in *Arctic-Subarctic Ocean Fluxes Defining the Role of the Northern Seas in Climate* (eds Dickson, R. R., Meincke, J. & Rhines, P.) 505–526 (Springer, 2008).
20. Lherminier, P. *et al.* Transports across the 2002 Greenland–Portugal OVIDE section and comparison with 1997. *J. Geophys. Res.* **112**, C07003 (2007).
21. Lherminier, P. *et al.* The Atlantic meridional overturning circulation and the subpolar gyre observed at the A25–OVIDE section in June 2002 and 2004. *Deep-Sea Res. I* **57**, 1374–1391 (2010).
22. Treguier, A. M. *et al.* The North Atlantic subpolar gyre in four high-resolution models. *J. Phys. Oceanogr.* **35**, 757–774 (2005).
23. Gourcuff, C., Lherminier, P., Mercier, H. & Le Traon, P. Y. Altimetry combined with hydrography for ocean transport estimation. *J. Atmos. Ocean. Technol.* **29**, 1324–1336 (2011).
24. Böning, C. W., Scheinert, M., Dengg, J., Biastoch, A. & Funk, A. Decadal variability of subpolar gyre transport and its reverberation in the North Atlantic overturning. *Geophys. Res. Lett.* **33**, L21S01 (2006).
25. Mikaloff-Fletcher, S. E. M. *et al.* Inverse estimates of anthropogenic CO₂ uptake, transport, and storage by the ocean. *Glob. Biogeochem. Cycles* **20**, GB2002 (2006).
26. Tjiputra, J. F., Assmann, K. & Heinze, C. Anthropogenic carbon dynamics in the changing ocean. *Ocean Sci.* **6**, 605–614 (2010).
27. Pérez, F. F. *et al.* Trends of anthropogenic CO₂ storage in North Atlantic water masses. *Biogeosciences* **7**, 1789–1807 (2010).
28. Hansen, B. & Østerhus, S. North Atlantic–Nordic Seas exchanges. *Prog. Oceanogr.* **45**, 109–208 (2000).
29. Tanhua, T., Olsson, K. A. & Jeansson, E. in *Arctic-Subarctic Ocean Fluxes Defining the Role of the Northern Seas in Climate* (eds Dickson, R. R., Meincke, J. & Rhines, P.) 475–503 (Springer, 2008).
30. Jutterström, S. *et al.* Evaluation of anthropogenic carbon in the Nordic Seas using observed relationships of N, P and C versus CFCs. *Prog. Oceanogr.* **78**, 78–84 (2008).
31. Anderson, L. G., Olsson, K. & Chierici, M. A carbon budget for the Arctic Ocean. *Glob. Biogeochem. Cycles* **12**, 455–465 (1998).
32. Olsen, A. *et al.* Magnitude and origin of the anthropogenic CO₂ increase and the ¹³C Suess effect in the Nordic Seas since 1981. *Glob. Biogeochem. Cycles* **20**, GB3027 (2006).
33. Körtzinger, A., Quay, P. D. & Sonnerup, R. E. Relationship between anthropogenic CO₂ and the ¹³C Suess effect in the North Atlantic Ocean. *Glob. Biogeochem. Cycles* **17**, 1005 (2003).
34. Kieke, D. *et al.* Changes in the pool of Labrador Sea Water in the subpolar North Atlantic. *Geophys. Res. Lett.* **34**, L06605 (2007).
35. Våge, K., Pickart, R. S., Moore, G. W. K. & Ribergaard, M. H. Winter mixed layer development in the central Irminger sea: The effect of strong, intermittent wind events. *J. Phys. Oceanogr.* **38**, 541–565 (2008).
36. Steinfeldt, R., Rhein, M., Bullister, J. L. & Tanhua, T. Inventory changes in anthropogenic carbon from 1997–2003 in the Atlantic Ocean between 20° S and 65° N. *Glob. Biogeochem. Cycles* **23**, GB3010 (2009).
37. Corbière, A., Metzl, N., Reverdin, G., Brunet, C. & Takahashi, T. Interannual and decadal variability of the oceanic carbon sink in the North Atlantic subpolar gyre. *Tellus B* **59**, 168–178 (2007).
38. Schuster, U. & Watson, A. J. A variable and decreasing sink for atmospheric CO₂ in the North Atlantic. *J. Geophys. Res.* **112**, C11006 (2007).
39. Visbeck, M. *et al.* The ocean's response to North Atlantic Oscillation variability. *Geophys. Monogr. Ser.* **134**, 113–145 (2003).
40. Schmitz, W. J. & Richardson, P. L. On the sources of the Florida Current. *Deep-Sea Res.* **38**, S389–S409 (1991).
41. Pérez, F. F. *et al.* Temporal variability of the anthropogenic CO₂ storage in the Irminger Sea. *Biogeosciences* **5**, 1669–1679 (2008).
42. Vázquez-Rodríguez, M. *et al.* Anthropogenic carbon distributions in the Atlantic Ocean: data-based estimates from the Arctic to the Antarctic. *Biogeosciences* **6**, 439–451 (2009).
43. Velo, A. *et al.* A multiparametric method of interpolation using WOA05 applied to anthropogenic CO₂ in the Atlantic. *Sci. Mar.* **74**, 21–32 (2010).
44. Touratier, F., Azouzi, L. & Goyet, C. CFC-11, $\Delta^{14}\text{C}$ and ³H tracers as a means to assess anthropogenic CO₂ concentrations in the ocean. *Tellus B* **59**, 318–325 (2007).

45. Waugh, D. W., Hall, T. M., McNeil, B. I., Key, R. & Matear, R. J. Anthropogenic CO₂ in the oceans estimated using transit time distributions. *Tellus B* **58**, 376–389 (2006).
46. Tanhua, T. *et al.* Ventilation of the Arctic Ocean: Mean ages and inventories of anthropogenic CO₂ and CFC-11. *J. Phys. Oceanogr.* **114**, C01002 (2009).
47. Daniault, N., Lherminier, P. & Mercier, H. Circulation and transport at the southeast tip of Greenland. *J. Phys. Oceanogr.* **41**, 437–457 (2011).
48. Jeansson, E. *et al.* The Nordic Seas carbon budget: Sources, sinks, and uncertainties. *Glob. Biogeochem. Cycles* **25**, GB4010 (2011).
49. Skjelvan, I. *et al.* in *The Nordic Seas: An Integrated Perspective Oceanography, Climatology, Biogeochemistry, and Modeling* (eds Drange, H. *et al.*) 157–175 (Geophys. Monogr. Ser., Vol. 158, AGU, 2005).

Acknowledgements

This work was supported by the Spanish Ministry of Sciences and Innovation and co-funded by the Fondo Europeo de Desarrollo Regional 2007–2012 (FEDER) through the CATARINA project (CTM2010-17141) and through EU FP7 project CARBOCHANGE ‘Changes in carbon uptake and emissions by oceans in a changing climate’, which received funding from the European Commission’s seventh Framework Programme EU under grant agreement no. 264879. The OVIDE research project

was co-funded by the IFREMER, CNRS/INSU and LEFE. H.M. was supported by CNRS and P.L. by IFREMER. M.V.-R. was funded by the CSIC I3P Predoctoral Grant program (I3P-BPD2005).

Author contributions

All authors contributed extensively to the work presented in this paper. F.F.P., H.M. and A.F.R. designed the research. F.F.P., H.M., M.V.-R., A.V., P.L. and A.F.R. analysed the physical and chemical data. H.M. and P.L. estimated the currents and thermohaline fields. F.F.P., M.V.-R., A.V. and G.R. determined the anthropogenic CO₂ concentrations and storage rates. H.M., F.F.P., P.L. and A.F.R. estimated the uncertainties. F.F.P., H.M., M.V.-R., P.C.P. and A.F.R. wrote the paper. All authors discussed the results and implications and commented on the manuscript at all stages.

Additional information

Supplementary information is available in the [online version of the paper](#). Reprints and permissions information is available online at www.nature.com/reprints. Correspondence and requests for materials should be addressed to F.F.P.

Competing financial interests

The authors declare no competing financial interests.